Quantitative investigation of polarization-dependent photocurrent in ferroelectric thin films

Komalika Rani, Sylvia Matzen, Stéphane Gable, Thomas Maroutian, Guillaume Agnus, Philippe Lecoeur

Quantitative investigation of polarization-dependent photocurrent in ferroelectric thin films

Komalika Rani, Sylvia Matzen, Stéphane Gable, Thomas Maroutian, Guillaume Agnus, Philippe Lecoeur

Université Paris-Saclay, CNRS, Centre de Nanosciences et de Nanotechnologies (C2N), 10 Boulevard Thomas Gobert, 91120 Palaiseau, France.

Abstract:

Ferroelectric thin films are investigated for their potential in photovoltaic (PV) applications, owing to their high open-circuit voltage and switchable photovoltaic effect. The direction of the ferroelectric polarization can control the sign of the photocurrent through the ferroelectric layer, theoretically allowing for 100% switchability of the photocurrent with the polarization, which is particularly interesting for photo-ferroelectric memories. However, the quantitative relationship between photocurrent and polarization remains little studied. In this work, a careful investigation of the polarization-dependent photocurrent of epitaxial $Pb(Zr,Ti)O_3$ thin films has been carried out, and has provided a quantitative determination of the unswitchable part of ferroelectric polarization. These results represent a systematic approach to study and optimize the switchability of photocurrent, and more broadly to get important insights on the ferroelectric behavior in all types of ferroelectric layers in which pinned polarization is difficult to investigate.

Introduction:

Ferroelectrics (FEs) are characterized by reversible spontaneous electric polarization, whose magnitude and direction can be precisely controlled by varying the temperature, composition, pressure, and electric field [1], enabling numerous applications including non-volatile ferroelectric memories [2]. In addition, the coupling between electric polarization and strain or magnetization makes ferroelectrics particularly interesting for the development of devices, such as sensors and actuators [3]. The study of light-matter interaction in FEs has shown the existence of novel phenomena, such as the unconventional photovoltaic effect [4-6] and the photostrictive effect (non-thermal photo-induced deformation) [7-10]. More recently, photo-ferroelectric materials have received renewed attention in thin films, offering rich physics and a wide range of exciting potential applications [11, 12]. In particular, the capability to tune photo-induced effects through the *in situ* control of electric polarization in FEs (tuning photocurrent [13, 14] or photostriction [15]) offers an additional degree of freedom in the control of materials functionalities with interesting applied perspectives [12, 16].

Ferroelectric thin films have a great potential in photovoltaic (PV) applications [11], owing to their high open-circuit voltage and switchable photovoltaic effect. The direction of the ferroelectric polarization can control the sign of the photocurrent in a ferroelectric thin film, theoretically allowing for 100% switchability of the photocurrent with the polarization, which is very interesting

for potential applications such as photo-ferroelectric memories. It has previously been demonstrated that the photocurrent follows a loop (as function of the poling voltage) similar to a ferroelectric hysteresis loop, indicating a direct relationship between photocurrent and electrically poled polarization for various ferroelectrics such as $BaTiO_3$ [17], $BiFeO_3$ [13], $Pb(Zr,Ti)O_3$ (PZT) [14, 17-19] and $PbTiO_3$-based solid solutions [20]. However, this relationship has not been directly studied quantitatively. Note that in a work on $BaTiO_3$ thin films [21], a linear relationship between photocurrent and remanent polarization has been evidenced, based on the decrease of polarization retention over time in a particular capacitor geometry, so without any classical control of the polarization state by electrical poling. Furthermore, the photocurrent switchability in integrated ferroelectric films between electrodes is not always achieved due to extrinsic parameters. For example, ferroelectric-electrode interfacial effects (Schottky barrier) [18, 22, 23], non-mobile charged defects, and the migration of charged defects, such as oxygen vacancies, under an applied electric field, can also affect the switchable photocurrent [11, 24, 25]. The mechanism of PV effect in ferroelectric thin films is thus complex and can include several contributions which are experimentally difficult to disentangle: the so-called bulk PV [26] effect related to the noncentrosymmetry in a FE, the presence of depolarizing field due to partially unscreened polarization, and the presence of built-in electric field in the material with various possible origins (such as gradient of charges, or Schottky potential barrier at interfaces giving a similar mechanism as classical PV effect in semiconductor p-n junctions).

In this work, a careful investigation of the polarization-dependent photocurrent of epitaxial lead zirconate titanate PZT thin films has been carried out. The purpose of this study is not to close the debate on the PV mechanisms in FE thin films, but to provide a more quantitative determination of the switchable vs unswitchable parts of photocurrent. More precisely, the dependence of the photocurrent as function of electrically controlled remanent polarization has been investigated. These measurements have shown that 1) the photocurrent depends linearly on the switchable part of the ferroelectric polarization and that 2) the analysis of this dependence provides important insights on the switchable and unswitchable internal electric fields in the FE material (the latter being necessarily related to pinned FE polarization). Such pinned polarization strongly affects the switchability of the PV properties in FEs and is otherwise rather difficult to probe by classical FE characterizations. These results are thus particularly relevant for the optimization of FE thin films, not only to achieve switchable PV properties but also to understand their ferroelectric response.

Methods:

Ferroelectric thin films of 100nm-thick $Pb(Zr_{0.2},Ti_{0.8})O_3$ (PZT) were grown epitaxially by pulsed laser deposition (PLD, KrF excimer laser, 248nm wavelength, $3J/cm^2$ fluence on target) on $SrTiO_3$(001) substrate (STO), with a 30nm-thick $SrRuO_3$ (SRO) bottom electrode. The SRO layer was deposited at 630°C under oxygen pressure of 120mTorr, with a growth rate of about 20 pulse/monolayer (ML). The PZT layer was further deposited at the same temperature under nitrous oxide (N_2O) pressure of 120mTorr, with a growth rate of about 15 pulse/ML. The crystal structure and surface morphology were studied using X-ray diffraction (XRD) and atomic force microscopy (AFM), which show excellent quality of the PZT (Figure S1, supporting information). Capacitor

structures of 100x100µm² were defined by optical lithography, deposition of 8nm-thick Pt top electrodes by sputtering and lift-off processes. Ferroelectric measurements were performed by measuring dynamic P-V hysteresis loop using a TFAnalyzer1000 (aixACCT systems). Photovoltaic measurements were performed using Keithley 2636 under UV illumination at 365 nm wavelength, corresponding to photon energy above the bandgap of PZT. By considering the onset of the measured photocurrent around 375nm (Figure S2, supporting information), a bandgap energy of around 3.3eV can indeed be approximated in our thin films. The samples were illuminated from the top with a diode of 365nm wavelength. Figure 1(a) depicts a sketch of the measurement setup of the Metal-Ferroelectric-Metal (MFM) device integrated into capacitor geometry, with a PZT thin film sandwiched between top Pt and bottom SRO electrode on the STO substrate. The incident power of diode on the capacitor device was measured to be 35.5mW/cm^2, of which 45% is absorbed by the Pt top electrode. A voltage pulse protocol, based on 0.5ms width triangular pulses, was used before each photovoltaic measurement to pole the device and reach a precise polarization state. Then, after each measurement under light illumination, another voltage pulse was applied in order to extract the remanent polarization value. The voltages were applied to the top electrode with the bottom electrode grounded and all the measurements were performed at room temperature.

Results & discussion:

Figure 1(b) depicts the ferroelectric polarization loop and its corresponding current loop, measured following the classical PUND (Positive Up Negative Down) method in order to remove the contribution from leakage currents. This contribution was rather small as can be seen from the similarity between the PUND loop and a classical ferroelectric loop (shown in Figure S3, supporting information). The PUND ferroelectric loop exhibits remanent polarizations of ±70µC/cm^2 and coercive voltage values of -2.7V and +3.3V.

Figure 1(c) depicts the photovoltaic properties of the PZT capacitor in the dark and under UV illumination at 365nm. The photocurrent was measured in the UP (P_{up}) and DOWN (P_{down}) states, corresponding to -6V and +6V poling voltage, respectively. The short-circuit photocurrent density (J_{sc}) for the P_{up} polarization state is positive, while the J_{sc} for the P_{down} polarization state is negative. This is consistent with the expected sign of photocurrent if we consider the depolarizing field as the main driving force. For P_{up} state for example, the depolarizing field would point towards the SRO bottom electrode. Under illumination, photo-generated electron-hole pairs would then be separated by this electric field, resulting in a positive photocurrent in short-circuit condition. By changing the polarization direction, the photocurrent changes sign, as previously reported in many studies. Naturally, for one given polarization state, the J_{sc} and the open-circuit voltage (V_{oc}) have opposite signs, since in open-circuit condition the photo-generated charges accumulate at each interface, tending to compensate the depolarizing field. However, this observed switchability of J_{sc} and V_{oc} could also come from the bulk PV effect. Note that J_{sc} and V_{oc} are slightly higher in absolute value for the P_{down} state (-51.6µA/cm^2 and 0.53V instead of 38.2µA/cm^2 and -0.4V for P_{up} state), which means that the switchable measured remanent polarization cannot fully explain the photovoltaic properties in these PZT thin films. The ferroelectric loop (Figure 1(b)) presents an imprint towards the positive voltage, indicating some internal electric field pointing up which could favor higher negative J_{sc}.

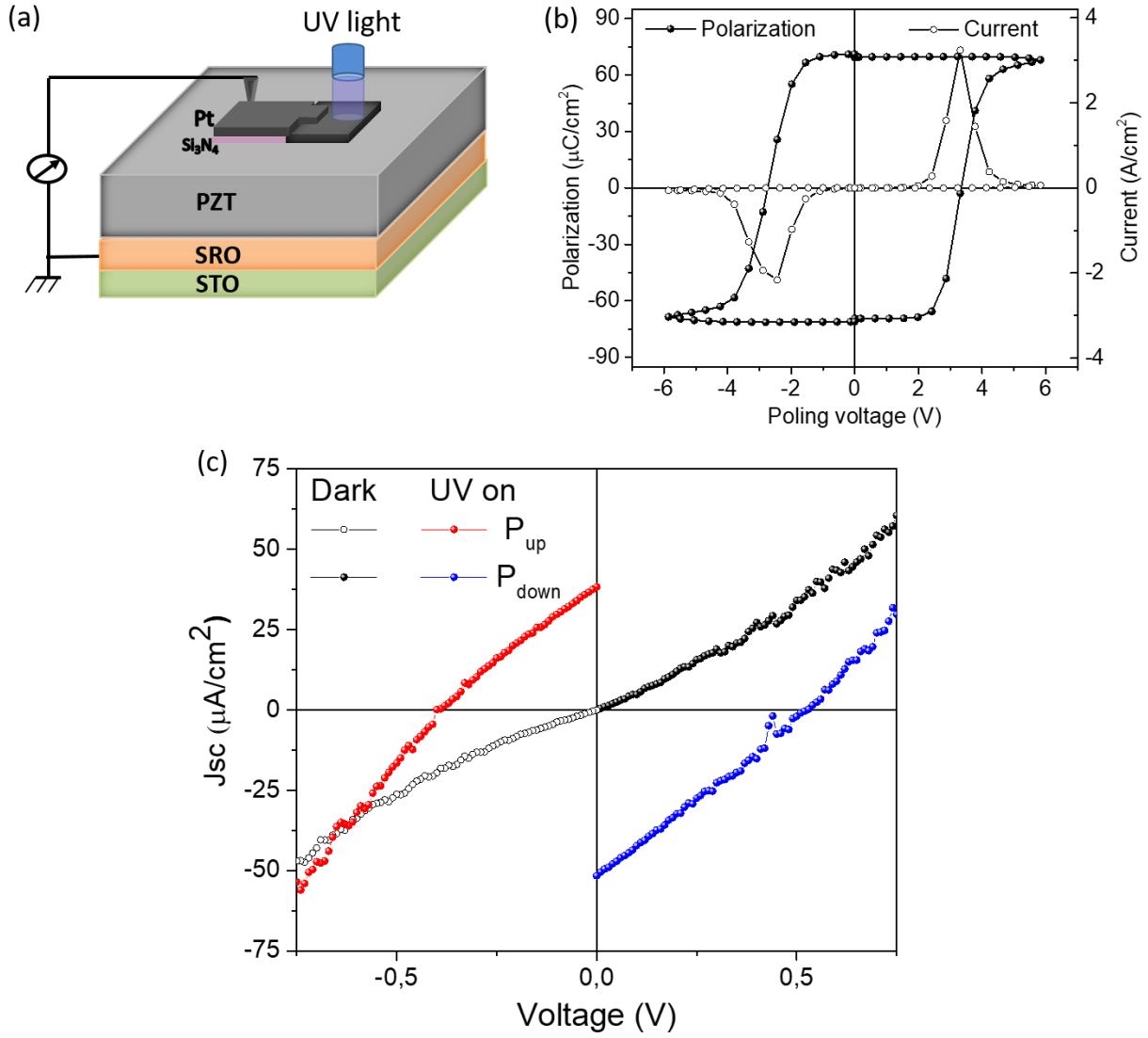

Figure1. (a) Setup for photocurrent measurements. (b) Ferroelectric hysteresis and corresponding current hysteresis loop for PZT thin film. (c) I-V measurement both in the dark and under UV illumination for UP and DOWN poling states.

A measurements protocol has been developed to pole the device and reach different well-defined polarization states in the PZT thin films. This is described in detail in supporting information and also shown in Figure 2. The triangular voltage waveform shown in Figure 2(a) consists of a writing pulse sequence to pole the sample before photocurrent measurements to precisely control its ferroelectric polarization state. This poling allows to achieve intermediate polarization ($P_{initial}$) between P_{up} and P_{down}. Figure 2(b) shows examples of a ferroelectric loops from the writing sequence, following the mentioned waveform from P_{down} to P_{up} polarization state and ending at particular and well-defined intermediate states. After the photocurrent measurements, a reading pulse sequence is used to measure the polarization state (P_{final}). The method to extract this final

remanent polarization value is further described in supporting information. It has been shown that the remanence of polarization is good for the different polarization states ($P_{initial}$~P_{final}) at the timescale of the measurements. In the rest of the article, the results will refer to P_{final} as remanent polarization values.

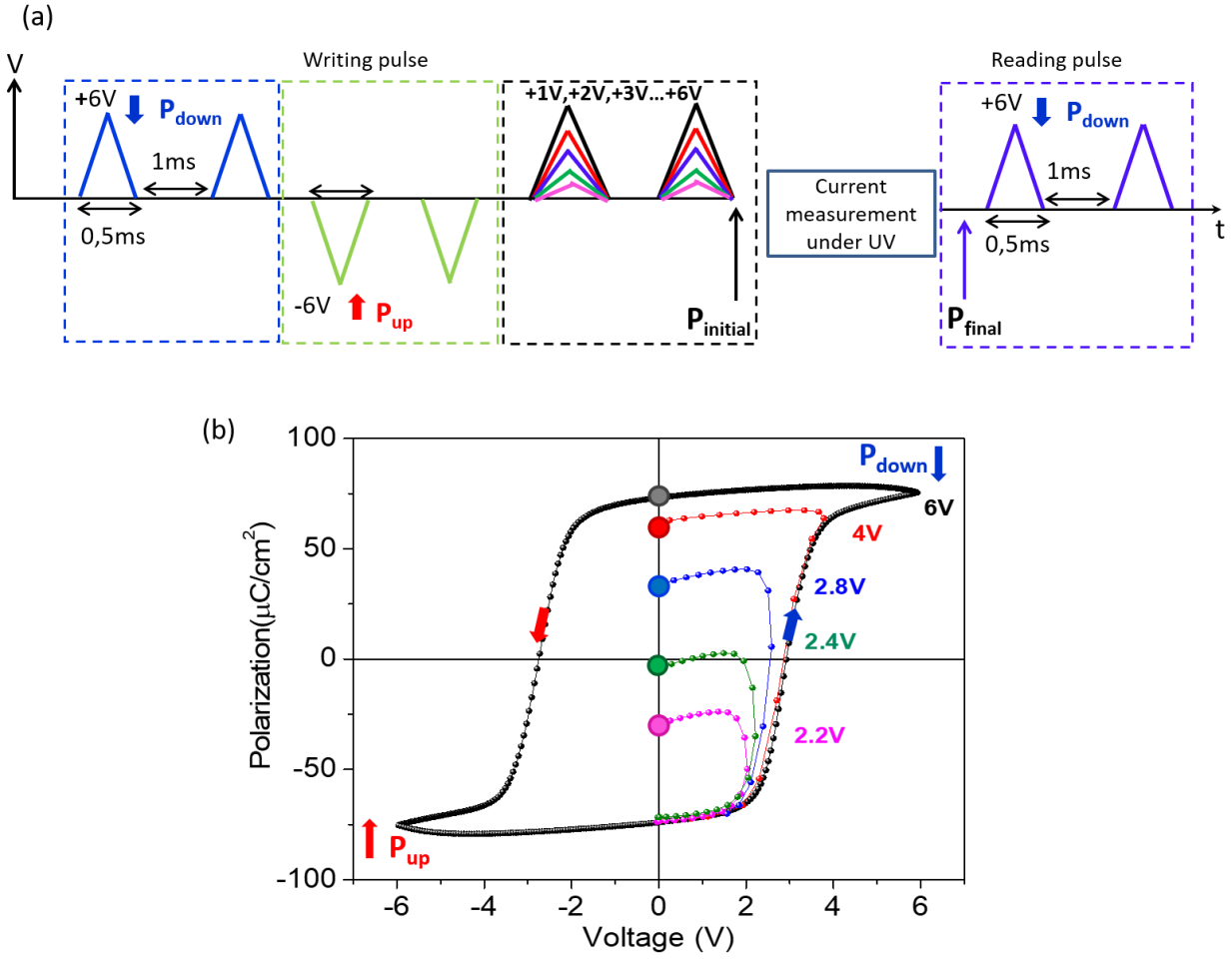

Figure 2. (a) Protocol for photocurrent measurements as function of different remanent polarization states. Writing pulse sequence used to pole the sample in particular polarization state and reading pulse used to extract the remanent polarization values after each photocurrent measurement. (b) Ferroelectric loop obtained by the writing pulse sequence, showing poling in different states.

Figure 3 shows steady-state short-circuit photocurrent measured at various intermediate poling states in dark and under illumination. A multistate switchable photocurrent can be achieved, like it was reported in $PbTiO_3$-based solid solutions ceramics [20]. These measurements agree well with the I(V) measurements in Figure 1 giving negative J_{sc} for P_{down} state, positive J_{sc} for P_{up} state and a highest J_{sc} in absolute value for P_{down} state. J_{sc} changes sign along the intermediate states when the poling voltage V_p is close to 2.4V. Similar measurements (not shown) have also been performed by starting with the P_{down} state (+6V poling) and progressively switching the polarization until the P_{up} state (-6V poling).

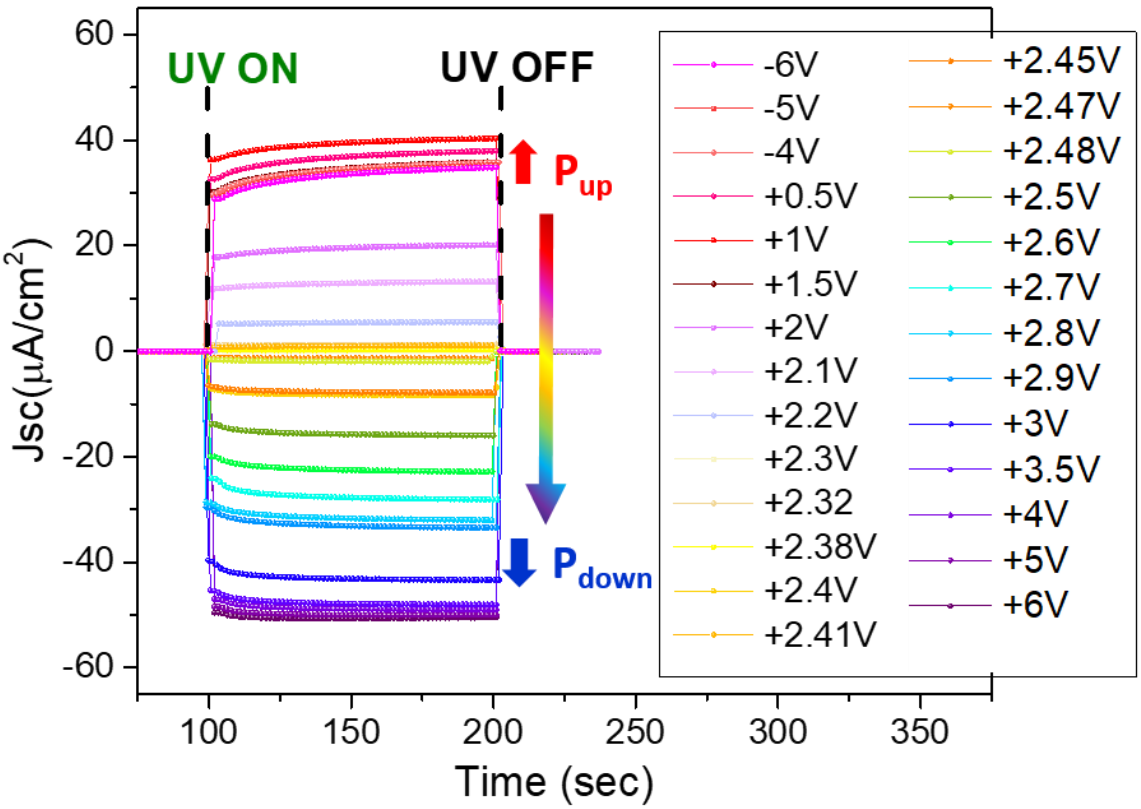

Figure 3. Time-dependent J_{sc} under UV ON and OFF condition for -6V poling (P_{up} state), +6V poling (P_{down} state) and different intermediate polarization states (while partially switching the polarization from P_{up} to P_{down} by applying positive poling voltage V_p.

The J_{sc} value measured right before switching off the illumination for each poling state was extracted and plotted as a function of poling voltage V_p in Figure 4. The J_{sc}-V_p curve clearly follows a hysteresis loop. In addition, after each photocurrent measurement, the final remanent polarization P_r=P_{final} was extracted using the previously mentioned protocol (more information in the supporting information) and plotted against the poling voltage. P_r-V_p follows a ferroelectric hysteresis loop, plotted in black in Figure 4, which, like the PUND polarization loop, also exhibits an asymmetry in coercive voltage towards positive values (V_p=-2.1V and +2.4V). However, the maximum and minimum P_r values for both +6V and -6V poling voltages are comparable (+67μC/cm² and -70μC/cm²), which indicates that the same amount of polarization can be poled up and down with good remanence. The P_r-V_p loop exhibits the same "coercive" poling voltage as for the photocurrent loop, indicating that the remanent polarization (P_r) and the short-circuit photocurrent (J_{sc}) are closely related. In this work, the similarity between both loops is remarkable and much stronger than in previous studies reported in the literature [13, 14, 17, 19, 20]. Indeed, it is evidenced here that the photocurrent loop is not to be compared with a classical ferroelectric

hysteresis loop but rather to the loop of the remanent polarization which is measured for each poling voltage.

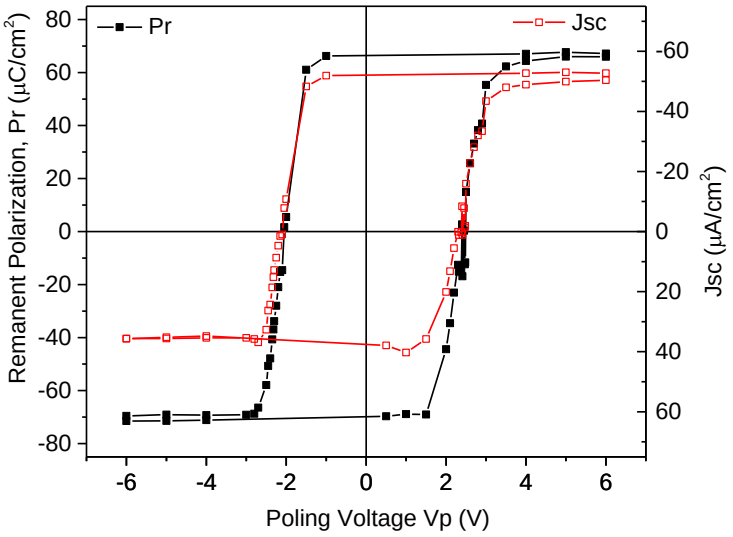

Figure 4. Loop of measured remanent polarization (P_r) and short-circuit photocurrent (J_{sc}) loop plotted as function of the poling voltage (V_p), showing similar hysteretic shape.

To study quantitatively the relationship between P_r and J_{sc}, J_{sc} was plotted as function of P_r in Figure 5. The linear dependence between P_r and J_{sc} is conspicuous over the whole range of polarization states. Note that the P_r values are remanent polarization values, which can only be measured by switching the polarization. From the polarization measurements alone, there is thus no way to evidence the possible presence of a polarization which cannot be switched during the pulse sequence. The observed experimental dependence in Figure 5 clearly proves that the short-circuit photocurrent J_{sc} is proportional to the total ferroelectric polarization in the ferroelectric devices. The fact that J_{sc} reaches zero for a non-zero P_r value demonstrates thus the presence of a non-switchable polarization part (P_{NS}) in the film. This P_{NS} contribution to the total polarization in the film can be quantitatively obtained from the J_{sc}-P_r measurements. J_{sc} equals zero for a measured P_r of -12μC/cm², meaning that P_{NS} is positive (pointing down) and equals 12μC/cm². This pinned part of polarization is in agreement with the asymmetry of the polarization loop which suggested an internal electric field pointing up [27]. The presence of this P_{NS} part explains thus why higher J_{sc} is measured in absolute value in the P_{down} state. In the +6V state, both P_{NS} and P_r add up, reaching a total equivalent polarization P_{tot} of +79μC/cm² pointing down, while in the -6V state, P_{tot} is smaller and reaches only -58μC/cm². The detailed investigation performed here on the photocurrent is thus a very powerful experimental method to access quantitatively the switchable behavior of the polarization in a ferroelectric thin film.

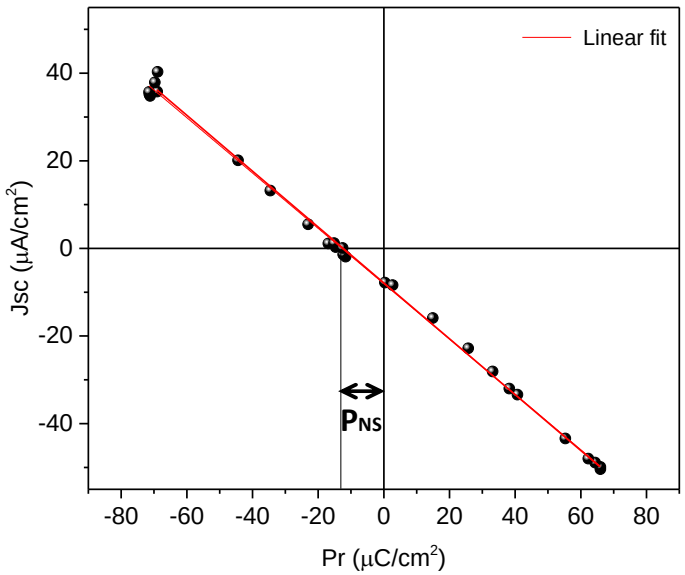

Figure 5. Linear dependence of photocurrent (J_{sc}) with the measured remanent polarization (P_r) in Pt/PZT/SRO-based capacitor device. J_{sc} reaching zero for a non-zero P_r value evidences the existence of a non-switchable polarization (P_{NS}) within the film.

Now, the linear relationship between J_{sc} and P_r could be explained rather by the bulk PV mechanism and/or by the presence of an internal field in the film proportional to P_r with opposite sign. This second mechanism will be tested in the rest of the article, in a similar way as done in [21]. The depolarizing field, which opposes the polarization, is related to the incomplete screening at the ferroelectric-electrode interfaces. Mehta *et al.* proposed a classic model for depolarization in ferroelectrics with metal electrodes in 1970 [28]. With the screening effect and the depolarization field, many models were proposed in which screening charges were dependent not only on electrodes but also on the properties of ferroelectric films [29] [30]. From the experimental results of the current study, J_{sc} can be written as $J_{sc}=J_S+J_{NS}$, where J_S is the switchable part of short-circuit photocurrent and J_{NS} the non-switchable part (J_{NS}=-8μA/cm²). J_S is thus experimentally proportional to the switchable remanent polarization (P_r). P_r can be related to the presence of a depolarizing field $E_{dep}=-\alpha P_r/\varepsilon$ [28], with ε the dielectric permittivity of the ferroelectric layer and α the fraction of unscreened switchable polarization. J_S can be expressed as $J_S=\sigma E_{dep}$ with σ the photoconductivity. In this picture, the relationship $J_S= - \sigma \alpha P_r/\varepsilon$ would then account for the experimental proportionality between J_s and P_r. However, this assumes that both ε and σ are the same in different P_r states, which is not the case as shown in Figure 6. In a ferroelectric layer, the dielectric constant is known to follow a butterfly loop as function of DC voltage with maximum values at the ferroelectric switching (Figure 6(a)). To take into account the dependence of the dielectric constant with the polarization state, capacitance has been measured in short-circuit condition and under light illumination for each intermediate P_r states. The dielectric constant, plotted as function of P_r in Figure 6(b), shows maximum values achieved when the polarization is close to zero and the values change by 27% in the whole P_r range. The photoconductivity σ was

also measured from the slope of I-V curves in the +0.1V/-0.1V range for each Pr state (Figure 6(c)). σ decreases for increasing positive P_r values (P_{down} state) and changes by 48% in the whole P_r range. Note that the same voltage protocol (Figure 2(a)) was used to pole the sample in the different intermediate P_r states before measuring the photocurrent (Figure S6, supporting information), the capacitance in short-circuit condition and under light illumination, and the photoconductivity to get a complete data set. P_r was further measured using the reading pulse sequence of the protocol. The dependence of both ε and σ with the polarization state could invalidate the model of depolarizing field to account for the linear relationship between J_{sc} and P_r. For each P_r state, corresponding ε and σ values have thus been considered and the $J_S \varepsilon / \sigma$ product has been plotted as function of P_r (Figure 6(d)). $J_S \varepsilon / \sigma$ does still appear proportional to P_r, so the model of depolarizing field cannot be discarded as origin of the photocurrent in these films in favor of the bulk PV effect. The linear fit of $J_S \varepsilon / \sigma$ as function of P_r gives a slope which is directly the opposite of the fraction of unscreened polarization α. A value of α=0.015 is obtained which is in agreement with the expected order of magnitude for screening efficiency [28] and consistent with the value reported for $BaTiO_3$ [21]. From this value of α, an effective depolarizing field of $-\alpha P_r/\varepsilon$ can be estimated and is found to be 85kV/cm, corresponding to 0.85V, for P_r=70μC/cm² and ε_r=140. In case of bulk PV effect, V_{oc} larger than corresponding depolarizing field can be achieved. Here, the open-circuit voltage reaches only 0.52V maximum, which is below 0.85V. In conclusion of this part, from the obtained experimental data, bulk PV as well as depolarizing field models can both be at the origin of the measured photocurrent in these PZT thin films.

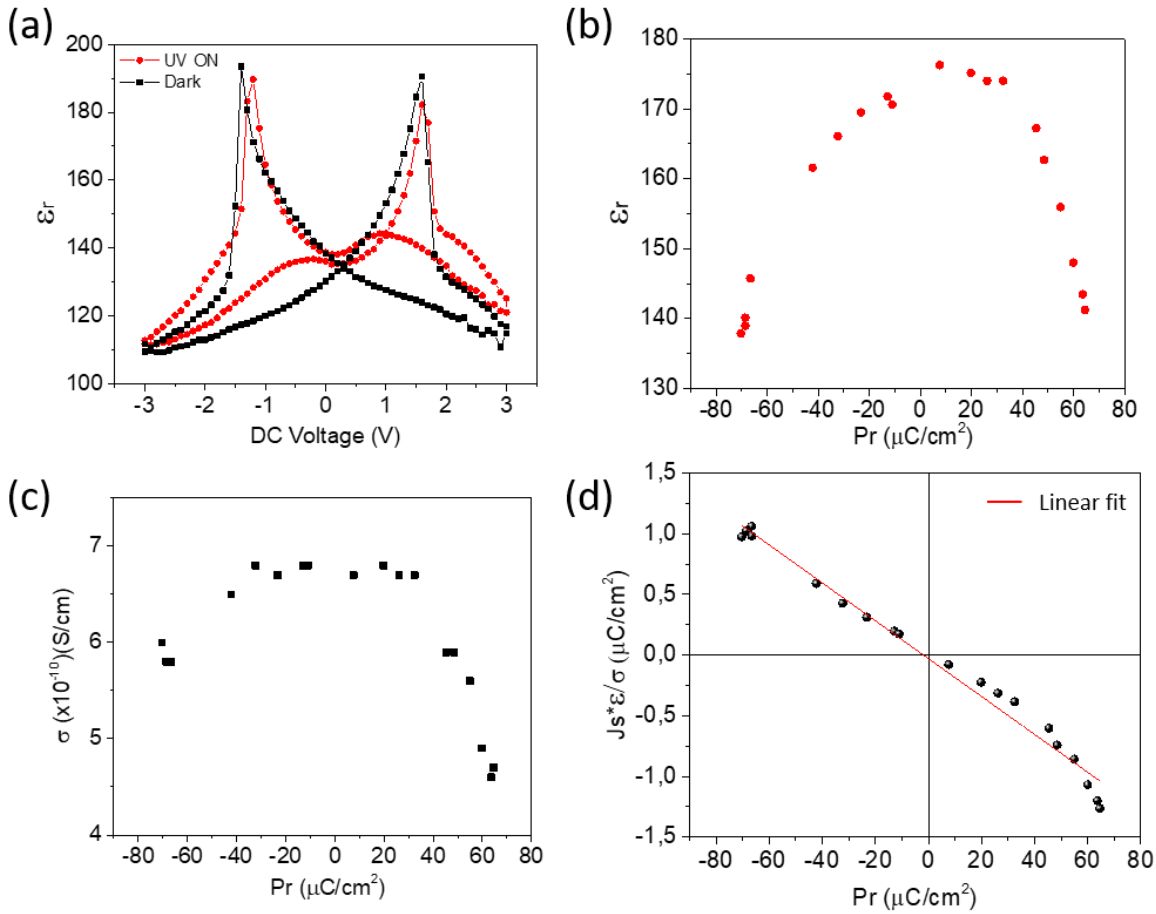

Figure 6: (a) Dielectric constant measured as function of DC voltage (using AC voltage of 30 mV and 1 kHz) in dark and under illumination conditions. The bumps observed under illumination before the ferroelectric switching happen when the resistivity is maximum (for DC voltage ~Voc) and could be related to space charge effects at interfaces. (b) Dielectric constant as function of P_r state measured under illumination. (c) Photoconductivity as function of P_r. (d) $J_S \varepsilon / \alpha$ values plotted as function of P_r.

Conclusion:

In conclusion, the short-circuit photocurrent has been measured in PZT epitaxial thin films for electrically written and stable intermediate remanent polarization states. A clear linear dependence between the photocurrent and the remanent polarization has been evidenced and the quantitative analysis of these results allowed to reveal the presence of a pinned part of polarization in the layer, which explains why the photocurrent is not 100% switchable by electrically poling the ferroelectric film. While the linear relationship could not help elucidating the origin of the photocurrent (which can be bulk PV and/or related to depolarizing field), the developed method is useful to reveal unswitchable part of polarization in a ferroelectric layer. It thus provides important insights on the ferroelectric behavior in all types of ferroelectric layers, while the classical ferroelectric loop only

gives a partial picture of the switchable polarization. Pinned polarization could be related to defects, in particular at interfaces with electrodes [31]. So, this type of study of photocurrent as function of remanent polarization could serve as an efficient tool to characterize the quality of a ferroelectric film integrated in capacitor. Investigating different types of electrode materials would be interesting to find out how it will affect the part of unswitchable polarization and if different screening efficiencies can be achieved and quantified. This could also give some answers in the search for the origin of photovoltaic effect in ferroelectrics. In this particular research field of PV in ferroelectrics, the results presented here provide a general approach to study and optimize the switchability of photocurrent, which could have far-reaching implications for future photo-ferroelectric memory applications.

Acknowledgements:

Research at the Center for Nanoscience and Nanotechnology was supported by the French RENATECH network and by the French National Research Agency (ANR) - Project UP-DOWN (Project No. ANR-18-CE09-0026-04). We thank François Julien and Maria Tchernycheva from C2N for their help with the spectrometer setup used for the wavelength-dependent photocurrent measurements presented in supporting information.

References:

[1] Wadhawan V 2000 *Introduction to Ferroic Materials* (CRC Press)

[2] Scott J F 2000 *Ferroelectric Memories* vol 3 (Berlin, Heidelberg: Part of the Springer Series in Advanced Microelectronics book series)

[3] Uchino K 2010 *Ferroelectric devices* (Boca Raton: CRC Press)

[4] Chynoweth A G 1956 Surface Space-Charge Layers in Barium Titanate *Phys. Rev.* **102** 705–14

[5] Fridkin V M, Grekov A A, Kosonogov N A and Volk T R 1972 Photodomain effect in BaTiO3 *Ferroelectrics* **4** 169–75

[6] Glass A M, von der Linde D and Negran T J 1974 High-voltage bulk photovoltaic effect and the photorefractive process in $LiNbO_3$ *Appl. Phys. Lett.* **25** 233–5

[7] Tatsuzaki I, Itoh K, Ueda S and Shindo Y 1966 Strain Along c Axis of SbSI Caused by Illumination in dc Electric Field *Phys. Rev. Lett.* **17** 198–200

[8] Brody P S 1983 Optomechanical bimorph actuator *Ferroelectrics* **50** 27–32

[9] Poosanaas P, Tonooka K and Uchino K 2000 Photostrictive actuators *Mechatronics* **10** 467–87

[10] Kundys B, Viret M, Colson D and Kundys D O 2010 Light-induced size changes in BiFeO3 crystals *Nature Mater* **9** 803–5

[11] Paillard C, Bai X, Infante I C, Guennou M, Geneste G, Alexe M, Kreisel J and Dkhil B 2016 Photovoltaics with Ferroelectrics: Current Status and Beyond *Advanced Materials* **28** 5153–68

[12] Kundys B 2015 Photostrictive materials *Applied Physics Reviews* **2** 011301

[13] Lee D, Baek S H, Kim T H, Yoon J-G, Folkman C M, Eom C B and Noh T W 2011 Polarity control of carrier injection at ferroelectric/metal interfaces for electrically switchable diode and photovoltaic effects *Phys. Rev. B* **84** 125305

[14] Pintilie L, Vrejoiu I, Le Rhun G and Alexe M 2007 Short-circuit photocurrent in epitaxial lead zirconate-titanate thin films *Journal of Applied Physics* **101** 064109

[15] S. Matzen, L. Guillemot, T. Maroutian, S. K. K. Patel, H. Wen, A. D. DiChiara, G. Agnus, O. G. Shpyrko, E. E. Fullerton, D. Ravelosona, P. Lecoeur, and R. Kukreja 2019 Tuning Ultrafast Photoinduced Strain in Ferroelectric-Based Devices *Advanced Electronic Materials* **5**, 1800709.

[16] Guo R, You L, Zhou Y, Shiuh Lim Z, Zou X, Chen L, Ramesh R and Wang J 2013 Non-volatile memory based on the ferroelectric photovoltaic effect *Nat Commun* **4** 1990

[17] Micheron F 1978 Dependence of the photovoltaic effect upon polarization in oxygen octaedra ferroelectrics *Ferroelectrics* **21** 607–9

[18] Yang Y S, Lee S J, Yi S, Chae B G, Lee S H, Joo H J and Jang M S 2000 Schottky barrier effects in the photocurrent of sol–gel derived lead zirconate titanate thin film capacitors *Appl. Phys. Lett.* **76** 774–6

[19] Cheng S, Fan Z, Zhao L, Guo H, Zheng D, Chen Z, Guo M, Jiang Y, Wu S, Zhang Z, Gao J, Lu X, Zhou G, Gao X and Liu J-M 2019 Enhanced photovoltaic efficiency and persisted photoresponse switchability in $LaVO_3/Pb(Zr_{0.2}Ti_{0.8})O_3$ perovskite heterostructures *J. Mater. Chem. C* **7** 12482–90

[20] Wu L, Burger A M, Bennett-Jackson A L, Spanier J E and Davies P K 2021 Polarization-Modulated Photovoltaic Effect at the Morphotropic Phase Boundary in Ferroelectric Ceramics *Adv. Electron. Mater.* **7** 2100144

[21] Liu F, Fina I, Gutiérrez D, Radaelli G, Bertacco R and Fontcuberta J 2015 Selecting Steady and Transient Photocurrent Response in $BaTiO_3$ Films *Advanced Electronic Materials* **1** 1500171

[22] Fang L, You L, Zhou Y, Ren P, Shiuh Lim Z and Wang J 2014 Switchable photovoltaic response from polarization modulated interfaces in $BiFeO_3$ thin films *Appl. Phys. Lett.* **104** 142903

[23] Pintilie L, Dragoi C and Pintilie I 2011 Interface controlled photovoltaic effect in epitaxial $Pb(Zr,Ti)O_3$ films with tetragonal structure *Journal of Applied Physics* **110** 044105

[24] Bai Z, Geng W, Zhang Y, Xu S, Guo H and Jiang A 2017 The abnormal photovoltaic effect in BiFeO3 thin films modulated by bipolar domain orientations and oxygen-vacancy migration *Appl. Phys. A* **123** 561

[25] Gao R. L., Yang H. W., Chen Y. S., Sun J. R., Zhao Y. G. and Shen B. G. 2014 Oxygen vacancies induced switchable and nonswitchable photovoltaic effects in $Ag/Bi_{0.9}La_{0.1}FeO_3/La_{0.7}Sr_{0.3}MnO_3$ sandwiched capacitors *Appl. Phys. Lett*. **104**, 031906.

[26] Fridkin V. M. 1979 Photoferroelectrics , *Springer-Verlag* (Berlin)

[27] Setter N., Damjanovic D., Eng L., Fox G. Gevorgian S., Hong S., Kingon A., Kohlstedt H., Park N. Y., Stephenson G. B., Stoltchnov I., Tagantsev A. K., Taylor D. V., Yamada T., Streiffer S. 2006 Ferroelectric thin films: Review of materials, properties, and applications *Journal of Applied Physics* **100**, 051606

[28] Mehta R R, Silverman B D and Jacobs J T 1973 Depolarization fields in thin ferroelectric films *Journal of Applied Physics* **44** 3379–85

[29] Batra I P, Wurfel P and Silverman B D 1973 Phase Transition, Stability, and Depolarization Field in Ferroelectric Thin Films *Phys. Rev. B* **8** 3257–65

[30] Glinchuk M D, Zaulychny B Y and Stephanovich V A 2005 Depolarization Field in Thin Ferroelectric Films With Account of Semiconductor Electrodes *Ferroelectrics* **316** 1–6

[31] Han M.-G., Marshall M. S. J., Wu L., Schofield M. A., Aoki T., Twesten R., Hoffman J., Walker F. J., Ahn C. A. and Zhu Y. Interface-induced nonswitchable domains in ferroelectric thin films 2014 *Nature Communications* **5**, 4693